Modeling and identification of an RRR-robot

Please check the document version of this publication:

Proceedings of the 40th IEEE
Conference on Decision and Control
Orlando, Florida USA, December 2001

TuP10-2

Modeling and Identification of an RRR-robot

[1]Dragan Kostić, [2]Ron Hensen, [3]Bram de Jager and [4]Maarten Steinbuch

Control System Technology Group, Faculty of Mechanical Engineering,

Eindhoven University of Technology (TU/e), P.O. Box 513, 5600 MB Eindhoven, The Netherlands

{[1]D.Kostic@tue.nl, [2]R.H.A.Hensen@tue.nl, [3]A.G.de.Jager@wfw.wtb.tue.nl and [4]M.Steinbuch@tue.nl}

Abstract

A dynamic model of a robot with 3 rotational degrees of freedom is derived in closed form. A systematic procedure for estimation of model dynamic parameters is suggested. It consists of the following steps: (i) identification of friction model parameters for each joint; (ii) calculation of optimal exciting trajectories, required for estimation of the remaining dynamic model parameters; (iii) estimation of these parameters using a least-squares method. The estimated model satisfactory reconstructs experimental control signals, justifying its use in model-based nonlinear control.

Keywords: Robotics, Modeling, Identification

1. Introduction

1.1.Modeling of robot dynamics and friction effects

An industrial-like direct-drive RRR robot, designed and installed in the Dynamics & Control Laboratory at TU/e, is used for evaluation of robot controllers [1,2]. It is especially convenient for testing a variety of advanced nonlinear control strategies, contributing to faster and more accurate robot motions. Among others, model-based control strategies are considered. They use an already known model of the robot dynamics [3] to compensate for nonlinear dynamic effects (e.g., Coriolis/centripetal, gravitational, and friction forces). To facilitate the use of a model-based control approach, the robot has been described with a detailed dynamic model, derived using the Lagrange-Euler formulation. The model is expressed in closed-form, such that each aspect of the dynamics (inertial, Coriolis/centripetal and gravitational effects) is available for analysis and manipulation.

For practical implementation of model-based control, friction in the joints should be taken into account, as it affects the quality of motion control [4]. To compensate for the friction, its dynamics can be modeled and estimated [4-7] and the resulting model is used for on-line compensation. There exists static and dynamic friction models [4]. Static models primarily describe friction effects in the sliding regime: Coulomb and viscous friction, Stribeck effect, frictional lag, position dependency. They are implemented using mathematical functions and/or look-up tables. Relevant models are usually complex, since diverse friction effects are described by different functions and switching between them is required at time instances when some effect becomes dominant [4]. This complicates their practical use. Dynamic friction models can describe friction dynamics in both pre-sliding and sliding regimes, not requiring additional switching logic. They are formed of differential equations, allowing more flexibility in "shaping" the friction behavior during the different regimes of motion. In this paper the LuGre friction model [5] is used. It suitably describes various friction effects with moderate mathematical complexity.

1.2.Estimation of dynamic parameters and model validation

Satisfactory results of model-based control depend not only on the relevancy of the implemented models, but also on the accuracy of parameters in the models. In this paper we conceptually suggest a systematic procedure for parameter estimation. Parameters describing kinematics [8] of the RRR robot – twist angles between each pair of adjacent joint axes and links lengths, are known from manufacturer data with sufficient accuracy. Inertial parameters of each link: mass, Cartesian coordinates of the center of mass, inertia tensor, and a moment of inertia of the motor shaft with additional equipment mounted (e.g., slip rings and bearings), are not known and should be estimated from the reference link motions and joint torques. It is well-known that it is not possible to estimate all individual parameters, but rather their nonlinear combinations [9]. These combinations establish a set of uniquely identifiable parameters, called the base parameter set (BPS). The dynamic model is linear in these parameters which enables estimation of the BPS elements using the least-squares (LS) methods [10,11]. Basic friction models can also be represented linearly in their parameters, enabling simultaneous estimation of BPS elements and friction parameters [10,11]. Considered LuGre friction model does not admit a linear parameterization, but requires independent estimation. Therefore, the estimation of the robot dynamics is done in two steps: first, the parameters of the LuGre friction model are estimated for each joint separately, and then all BPS elements are simultaneously estimated. The LuGre model has a dynamic and a static part, each demanding individual estimation. Parameters of both parts are commonly estimated using time-consuming procedures in time-domain [4]. A frequency-domain method for estimation of the dynamic part is suggested in [7]. It is shown that this gives valid estimates, and much faster than in the time-domain approach. As such, it is used in our estimation concept. For estimation of the static part we compare the standard procedure [4] with a method using the augmented state Extended Kalman Filter (EKF) [6,12]. It occurs that the EKF method gives relevant estimates with less efforts involved, qualifying to be incorporated in our estimation concept. To estimate elements of the BPS, the robot actuators should be excited by control inputs enabling reliable and fast parameter estimation in the presence of disturbances (e.g., measurement noise). Guidelines to determine such excitations are available in [10,11], and are used in our estimation procedure. Excitations and resulting joint motions (positions, velocities and accelerations) are used in the LS estimation of the parameters of the symbolic dynamic model. To that model we add the LuGre friction models of all joints. Thus we establish a complete model applicable for model-based control. Experimental validation of the model is done as suggested in [10,11]. It satisfactorily reconstructs experimentally generated control signals, justifying its use in model-based control.

The paper is organized as follows. In the Section 2 kinematic and dynamic models of the RRR robot are given. Section 3 describes a methodology for friction identification, considering both pre-sliding and sliding regimes of the friction. In the Section 4 we present calculation of an optimal exciting trajectory, and estimation of the robot dynamic parameters. Final remarks are given in the last section.

2. Kinematics and dynamics of an RRR robot

An RRR robot has an anthropomorphic structure featuring the most dexterous and versatile motions, which is paid by highly nonlinear kinematic and dynamic behavior [3]. Direct drive actuation makes the control problem even harder, since there are no gear-heads to reduce the effects of nonlinear dynamics [2]. A kinematic diagram and a picture of the robot are shown in Fig. 1.
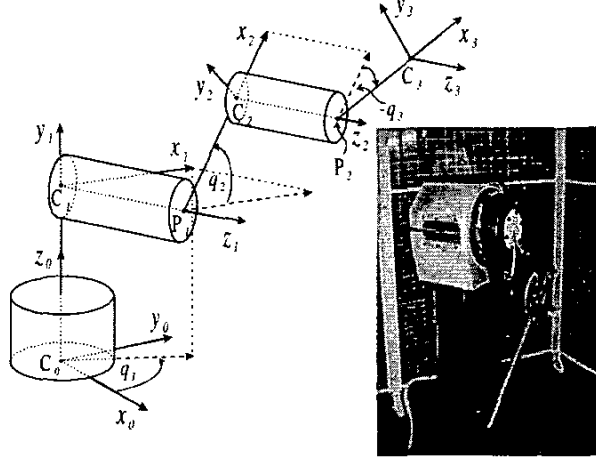

Fig. 1. Kinematic diagram and picture of the RRR robot

A coordinate frame is assigned to each joint according to the Denavit-Hartenberg (DH) notation [8], enabling a systematic description of the kinematics with minimal parameterization (Table 1). The joint angles q_i (i=1,2,3) are indicated in Fig. 1.

Table 1. DH parameters of the RRR robot

d.o.f.*	Link twist	Link length	Joint angle	Link offset
1	$\pi/2$	0	q_1	C_0C_1
2	0	P_1C_2	q_2	C_1P_1
3	0	P_2C_3	q_3	C_2P_2

*d.o.f. stands for "degree of freedom"

A dynamic model of the robot is derived using the Lagrange-Euler formulation [8]. The standard form of the model is:

$$D(q)\ddot{q} + c(q,\dot{q}) + h(q) = \tau , \qquad (1)$$

where q, $\dot{q}$ and $\ddot{q}$ are 3×1 vectors of joint positions, velocities and accelerations, respectively, D is a 3×3 inertia matrix, c and g are 3×1 vectors of Coriolis/centripetal respectively gravitational effects, and τ is a 3×1 vector of joint torques (excitations).

To provide a complete description of the robot dynamics, the behavior of joint actuators should be also taken into account. Joints of the RRR robot are actuated by brushless DC motors. Control signals u_i (i=1,2,3) from a DSP controller are amplified using a controlled current invertor [1], which provides a linear relation within the nominal operating range:

$$k_{t,i}u_i = \tau_i + J_{m,i}\ddot{q}_i \quad (i = 1,2,3) . \qquad (2)$$

$k_{t,i}$ denotes torque constant. Combining (1) and (2) gives:

$$u_i = \sum_{\substack{j=1 \\ j \neq i}}^{3} \ddot{q}_j \frac{d_{ij}(q)}{k_{t,i}} + \ddot{q}_i \frac{J_{m,i} + d_{ii}(q)}{k_{t,i}} + \frac{c_i(q) + h_i(q)}{k_{t,i}}, \qquad (3)$$

$i = 1,2,3$. $J_{m,i}$ denotes the inertia moment of the motor shaft.

The dynamic model was first derived in the form (3). Then it was rewritten to be linear in the BPS elements. This required determination of the minimum set of identifiable dynamic parameters. For the RRR robot there exists 15 such parameters. However, if the inertia moments $J_{m,i}$ are also unknown, then dimension of the BPS increases to 16. The minimal set of identifiable parameters is thus defined by:

$$p = [p_1 \quad p_2 \quad \cdots \quad p_{16}]^T , \qquad (4)$$

and the complete robot dynamics can be represented as:

$$k_t^{-1} \cdot R(q,\dot{q},\ddot{q}) \cdot p = u , \qquad (5)$$

$$u = [u_1 \quad u_2 \quad u_3]^T , \qquad (6)$$

$$k_t = diag[k_{t,1} \quad k_{t,2} \quad k_{t,3}] . \qquad (7)$$

The validity of the symbolic model is confirmed by comparing its inverse-dynamics solutions [8] with the solutions obtained using the Robotics Toolbox for Matlab [13]. Discrepancies are within numerical round-off.

In the real system friction affects the robot dynamics and can not be disregarded if high-performance motion control is required. Hence, we must introduce friction into the model (5):

$$u^n = u + u^f , \qquad (8)$$

where u is defined by (6), u^f represents friction effects and u^n total excitations that should be applied.

Friction phenomena are modeled using the LuGre friction model. The model has the form:

$$u_i^f = \sigma_{0,i}z_i + \sigma_{1,i}\dot{z}_i + \alpha_{2,i}\dot{q}_i ; \quad \dot{z}_i = \dot{q}_i - \sigma_{0,i}\frac{|\dot{q}_i|}{\gamma(\dot{q}_i)}z_i , \qquad (9)$$

where u_i^f is the voltage due to the friction, z_i is a pre-sliding deflection of materials in contact, and $\gamma(\dot{q}_i)$ is the Stribeck curve for steady-state velocities ($i = 1,2,3$). Dynamic (pre-sliding regime) model parameters are $\sigma_{0,i}$ and $\sigma_{1,i}$, denoting the stiffness of pre-sliding deflections and viscous damping of the deflections, respectively. The sliding regime corresponds to the static (steady-state) behavior of the model. The corresponding model is obtained from (9) by assuming constant velocity motion:

$$u_{ss,i}^f = \gamma(\dot{q}_i)\text{sgn}(\dot{q}_i) + \alpha_{2,i}\dot{q}_i ; \quad \gamma_i(\dot{q}_i) = \alpha_{0,i} + \alpha_{1,i}e^{-(\dot{q}_i/v_{s,i})^2} \qquad (10)$$

and features the following (static) parameters: $v_{s,i}$ is the Stribeck velocity, while $\alpha_{0,i}$, $\alpha_{1,i}$ and $\alpha_{2,i}$ are Coulomb, static and viscous friction coefficients.

3. Identification of the friction

3.1. Time-domain identification of static friction parameters

Static friction parameters are estimated for each joint independently. Time domain identification based on constant velocity experiments was applied in the case of the first two joints, following the guidelines presented in [4]. It consists of a sequence of individual experiments, each providing some of the static friction parameters. The estimates are presented in Table 2. Although straightforward and reliable, this procedure is not time

efficient. In order to make the estimation quicker, we prefer a simultaneous identification of all static friction parameters using an augmented state EKF [6,12]. Such procedure is successfully implemented for estimation of the third joint's static friction parameters. As motion control of the RRR robot is performed by means of a DSP-based digital controller [1,2] with a sampling period of 1 ms, the EKF for nonlinear continuous-time processes with discrete-time measurements was considered. The EKF algorithm is a recursive formulation that updates the estimates at discrete-time instants, i.e., when the outputs of the system are measured. The algorithm is given in [12], and has been already used for friction identification in [6].

Table 2. Estimated static friction parameters

i	$\alpha_{0,i}$ [V]	$\alpha_{1,i}$ [V]	$v_{s,i}$ [rad/s]	$\alpha_{2,i}$ [Vs/rad]
1	0.2285	0.0493	0.0031819	0.093557
2	0.35	0.07	0.003	0.07
3	0.3561	-0.1736	0.003	0.1252

Identification of the third joint's friction parameters is done with the first two joints standing still in some preferred position, by means of PD control feedback. The resulting dynamics of the robot is in fact dynamics of the third joint considered separately:

$$\ddot{q}_3 = [k_{t,3}(u_3^n - u_3^f) - l_3 \sin(q_3)]/J_3, \qquad (11)$$

where u_3^n and u_3^f are the joint excitation and the friction, J_3 is the equivalent moment of inertia of the load on the motor shaft, and l_3 is a coefficient. The torque constant $k_{t,3}$ is assumed known from the manufacturer data [1,2]. In the sliding regime, friction is described by (10), and we replace u_3^f in (11) by $u_{ss,3}^f$. This gives a nonlinear system with unknown parameters $\alpha_{0,3}$, $\alpha_{1,3}$, $v_{s,3}$, $\alpha_{2,3}$, J_3 and l_3. However, for a suitable excitation $u_3^n(t)$, we may measure the system response ($q_3(t)$ and $\dot{q}_3(t)$) and use it for Kalman filtering. The EKF simultaneously calculates estimates of the state coordinates (position and velocity) and unknown model parameters. To sufficiently excite all unknown parameters, we use a manually generated control sequence presented in Fig. 2, which has been successfully applied in [6]. The excitation was open loop, and the system responded as shown in Fig. 3. The response has slow and fast phases, to acquire enough information about the static friction parameters. The excitation and the response are then fed into an EKF. Filtering is done off-line. The filter is tuned, like explained in [6], and its transient dynamics required ten filter runs for all parameters to converge. Before each run, the estimated parameters are initialized by their final estimates from the previous run. The final estimates are presented in Table 2, except estimates of J_3 and l_3 which are equal to 0.0709 kgm^2, and 1.9688 Nm.

3.2. Frequency-domain identification of dynamic friction parameters

Dynamic friction parameters are identified according to the procedure suggested in [7]. This procedure is time efficient, requiring just a few experiments where the system is excited with random noise and the corresponding frequency response function (FRF) is measured. However, it requires position sensors of high resolution, since very small displacements have to be detected. Our experimental set-up has incremental encoders producing 655360

pulses per revolution, which is sufficient. Knowledge of the parameters obtained in the previous section is necessary.

If we linearize the LuGre friction model (9) around zero velocity and zero pre-sliding displacement, we can use (11) to obtain the following FRF:

$$H_i(s) = \frac{Q_i(s)}{U_i^n(s)} = \frac{1}{(J_i/k_{t,i})s^2 + (\sigma_{1,i} + \alpha_{2,i})s + \sigma_{0,i} + l_i/k_{t,i}}. \quad (12)$$

FRF describes robot dynamics in some predefined configuration where the i-th joint is excited with a random noise, while the other two joints are kept fixed using a PD control.
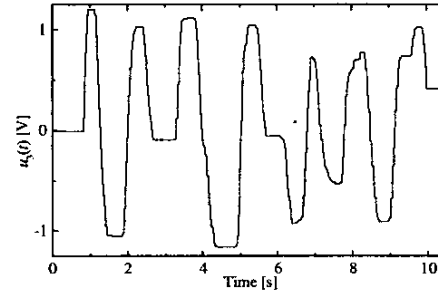

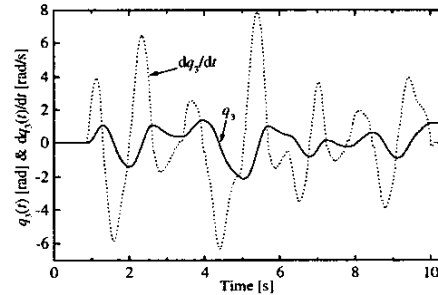Fig. 2. Control sequence exciting actuator of the third joint

Fig. 3. Response of the third joint to excitation shown in Fig. 2

Estimating the parameters in (12), using the already estimated J_i, $\alpha_{2,i}$ and l_i, gives the dynamic friction parameters $\sigma_{0,i}$ and $\sigma_{1,i}$. Each joint is excited with random noise of a bandwidth up to 200 Hz, with RMS below the static friction level to prevent leaving the pre-sliding region. $H_i(j\omega)$ is obtained by averaging 50 time series of 4096 samples at the sampling frequency of 1 kHz, with a Hanning window and 50 % overlap. In [7] it is explained that because the FRF (12) is valid only locally, we should consider the FRF obtained for the lowest noise level for which the pre-sliding behavior is observed. In case of the third joint, that corresponds to a RMS noise level of 2.5 mV. Experimental results for $H_3(j\omega)$ are presented in Fig. 4 with a solid line. The fitted curve is shown in Fig. 4 with a dashed line. The estimates for all three joints are presented in Table 3, which completes the estimation of the friction parameters.

3.3. Validation of the estimated friction model

The friction model is needed for identification of the BPS, and therefore it should be validated. For that purpose we do two tests. The first one should show how accurate the friction models reconstruct experimental system responses $q_i(t)$. For illustration, we present validation results for the third joint. Similar results are

obtained for the other joints. The dynamics (11), combined with the estimated friction model (9),(10), is solved for the excitation presented in Fig. 2. The simulated motion of the joint is shown in Fig. 5 by a dotted line, while the experimentally measured one is given by a solid line. We observe a perfect agreement.
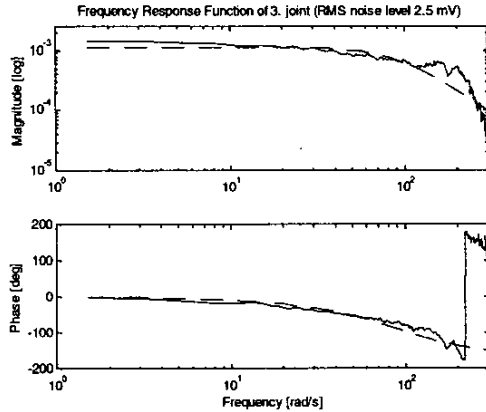

Fig. 4. Measured (solid) and estimated (dashed) Bode plots of the third joint's FRF

Table 3. Estimated dynamic friction parameters

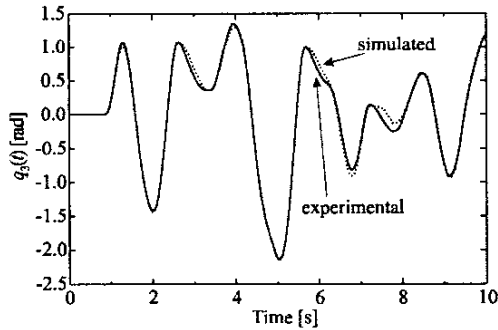| i	$\sigma_{0,i}$ [V/rad]	$\sigma_{1,i}$ [Vs/rad]
1	1170.6	3.6743
2	196	6.32
3	221.2	1.4832

Fig. 5. Validation of the estimated friction parameters

For the second test, the third joint is oriented vertically and downwards. Then, it was excited by a sinusoidal input, just to enable a gravity force to have effect on joint motion. The friction compensation using the identified model was active from the very beginning of the experiment. After some time, the sinusoidal excitation is switched-off, but the friction compensation remains active. Motion of the joint is governed by the equivalent dynamics (11), with u_3^n equal to the actual friction compensation. Since effects of the term u_3^f in (11) are compensated, and the joint features stable oscillations around the equilibrium, we obtain compensation adequate. The friction is also position dependent with a repetitive behavior during consecutive joint revolutions. The estimation of the BPS elements does not take the friction position dependency into account.

4. Identification of the robot dynamic model

In this section we work out the procedure which provides estimates of the minimum number of identifiable dynamic parameters. First, a brief description of the least-squares (LS) method for parameter estimation is given. The reason for this is twofold: (i) the theory underlying LS estimation is used for generation of excitations for identification experiments; (ii) estimates of dynamic parameters are obtained using the LS estimation method.

4.1. LS method

Consider the robot dynamic model (5). Let us excite joint actuators by some $u(t)$, and then record the resulting $q(t)$, $\dot{q}(t)$ and $\ddot{q}(t)$. Assume we have collected ζ samples of each element of u, q, $\dot{q}$ and $\ddot{q}$, corresponding to time instants $t_0, t_1, \ldots, t_{\zeta-1}$. Since (5) holds for each $t_k \in \{t_0, t_1, \ldots, t_{\zeta-1}\}$, we may form the following system of equations:

$$\Phi \cdot p = y, \qquad (13)$$

where

$$\Phi = \begin{bmatrix} k_t^{-1} \cdot R(q(t_0), \dot{q}(t_0), \ddot{q}(t_0)) \\ k_t^{-1} \cdot R(q(t_1), \dot{q}(t_1), \ddot{q}(t_1)) \\ \vdots \\ k_t^{-1} \cdot R(q(t_\zeta), \dot{q}(t_\zeta), \ddot{q}(t_\zeta)) \end{bmatrix}, \qquad (14)$$

$$y = [u^T(t_0), u^T(t_1), \ldots, u^T(t_\zeta)]^T. \qquad (15)$$

The control sequence $u(t)$ is appropriate if it sufficiently excites the robot dynamics. With such excitation, the vector of identifiable parameters p can be found using some generalized inverse of Φ:

$$p = \Phi^* \cdot y, \qquad (16)$$

where '*' denotes generalized matrix inverse [14].

To verify if the excitation used in the estimation of the unknown p is appropriate, one considers the cardinal number J_k of Φ. This is the ratio between maximal and minimal singular values of Φ [14]. If J_k is small, then Φ^* is less sensitive to disturbances, and estimates of p are more reliable. In the literature other criteria are also suggested [10,11], but here we use the cardinal number only. It is because choice of other criterion does not influence estimation concept we suggest.

4.2. Design of optimal excitation

The design of actuators' excitations yielding a small value of J_k is done as in [10,11]. The motion of each joint is postulated in the form of a five terms Fourier series to ensure cyclic motions during the estimation experiment. Cyclic motions are preferable, since they enable averaging of the measured data in order to reduce the influence of noise. A period of motions should be long enough to prevent a minimal singular value of IM to be close to zero. We use a period of 10 s, which agrees with the choices reported in [12,13]. Now, we search for coefficients of the terms in the Fourier series that give a small J_k, within the allowable range of joint velocities $|\dot{q}_1| \leq 2\pi$ rad/s, $|\dot{q}_2| \leq 3\pi$ rad/s, and $|\dot{q}_3| \leq 3\pi$ rad/s. It can be noticed that no restrictions were put on the joint positions. The use of slip rings for transfer of power and sensor signals via the robot joints enables an infinite range of motions in each d.o.f. [1,2].

The coefficients are found using a constrained optimization algorithm and substituted into the Fourier series to give the excitation trajectories presented in Fig. 6.

To implement optimal motions on the real system, we apply a PD controller to each d.o.f. separately

$$u_i^n = k_{p,i}(q_{i,ref} - q_i) + k_{d,i}(\dot{q}_{i,ref} - \dot{q}_i) \quad (i = 1,2,3), \quad (17)$$

where $q_{i,ref}$ corresponds to the trajectories shown in Fig. 6. The gains in (17) were tuned using 'trial and error', to ensure reasonable tracking with a low level of noise in the control inputs $\mathbf{u}^n(t)$ (excitations), as shown in Fig. 7.
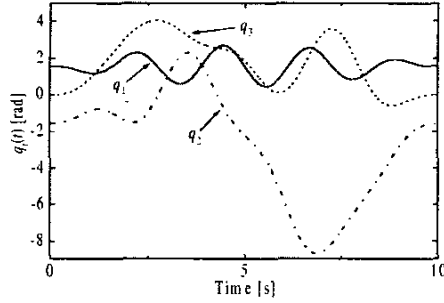

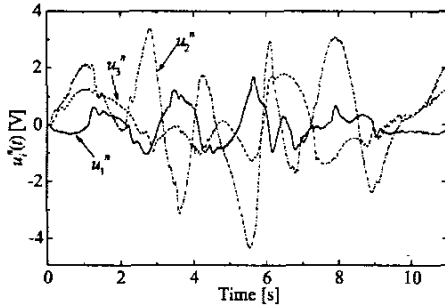Fig. 6. Joint trajectories optimizing cardinal number of IM

Fig. 7. Control inputs from the identification experiment

During the identification experiment, we recorded $\mathbf{u}^n(t)$ and $\mathbf{q}(t)$. As LS estimation procedure is performed off-line, $\dot{\mathbf{q}}(t)$ and $\ddot{\mathbf{q}}(t)$ are reconstructed using digital filtering (Euler differentiation + 'filtfilt' Matlab routine implementing 4th order Butterworth filtering). The velocities were then fed into the estimated friction models. The reconstructed friction effects are shown in Fig. 8. As demonstrated in the previous section, quality of reconstructed $\mathbf{u}^f(t)$ is sufficient to enable correction of experimental $\mathbf{u}^n(t)$, which gives the control voltage $\mathbf{u}(t)$ exciting the robot dynamics (5). Finally, $\mathbf{u}(t)$, $\mathbf{q}(t)$, $\dot{\mathbf{q}}(t)$ and $\ddot{\mathbf{q}}(t)$ are used in estimation of $\mathbf{p}$, which is presented next.

4.3. Estimation of the BPS elements

The sequences of $\mathbf{u}(t)$, $\mathbf{q}(t)$, $\dot{\mathbf{q}}(t)$ and $\ddot{\mathbf{q}}(t)$ are processed according to the procedure explained in Section 4.1. We used data measured at 10 ms intervals. In total, each signal contained 1094 samples. The cardinal number of Φ was 8.06, which was more than expected from the design phase. With more data samples we could achieve a lower J_k, however, with a higher computational burden due to an increased size of Φ.

Torque constants are assumed to be known, and are assigned according to the manufacturer data [1,2]:

$$\mathbf{k_t} = \text{diag}[12 \quad 6.3 \quad 3] \, [\text{Nm/V}] . \quad (18)$$

The applied LS estimation results in the convergence of all elements of $\mathbf{p}$, see the diagrams in Fig. 9.

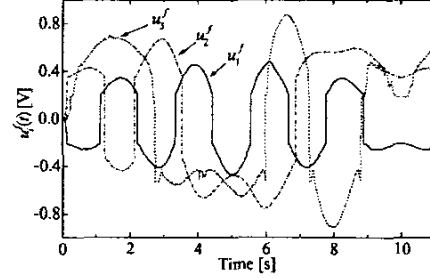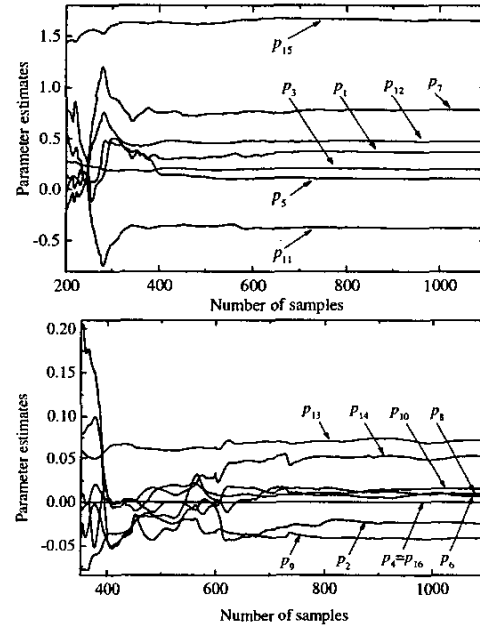
Fig. 8. Reconstruction of the friction effects

Fig. 9. Convergence of estimated parameters

The final set of parameters is given by:

$$p_1 = 0.3654, \; p_2 = -0.0235, \; p_3 = 0.2007, \; p_4 = 0,$$
$$p_5 = 0.1064, \; p_6 = 0.0077, \; p_7 = 0.7762, \; p_8 = 0.0105,$$
$$p_9 = -0.0415, \; p_{10} = 0.0148, \; p_{11} = -0.3713, \; p_{12} = 0.4738, \quad (19)$$
$$p_{13} = 0.0714, \; p_{14} = 0.0514, \; p_{15} = 1.6598, \; p_{16} = 0.$$

Parameters (19) together with those given in Tables 2 and 3, accurately describe the robot dynamics including friction (8).

To evaluate whether the model has sufficient prediction capability, it is tested in experiments of the following kind [10,11]. The motion task was defined by:

$$q_{ref,i}(t) = q_{ref,i}(0) + \pi \sin(2\pi t / 5) / 2 \quad (i = 1,2,3), \quad (20)$$

with the initial location

$$[q_{ref,1}(0) \; q_{ref,2}(0) \; q_{ref,3}(0)] = [\pi/2 \; -\pi/2 \; 0] . \quad (21)$$

The desired motions are implemented using the PD controllers

(17), and the resulting control sequences are measured. During the experiments we achieved small tracking errors between desired and executed joint trajectories. Hence, in order to prevent additional filtering of the acceleration signal, that was considerably corrupted by noise, we fed the estimated model (8) with the reference sequences $q_{ref}(t)$, $\dot{q}_{ref}(t)$ and $\ddot{q}_{ref}(t)$. In this way we try to reconstruct the actual voltages (17). The greatest discrepancy is observed in the first joint, and we present it in Fig. 10 as the worst case. Almost perfect reconstruction is obtained in the second joint, and a very good one in the third. Observed differences may be due to inaccurate values of adopted torque constants, unmodeled dynamics of DC actuators, unmodeled position dependency of the friction, or because of other unmodeled effects (e.g., cogging). It is also influenced by position errors between desired and actual experimental motions. However it can be disputed whether the purely deterministic identification, as applied, is appropriate for the given estimation problem where noise is prevalent. Nevertheless, the results are surprisingly good.
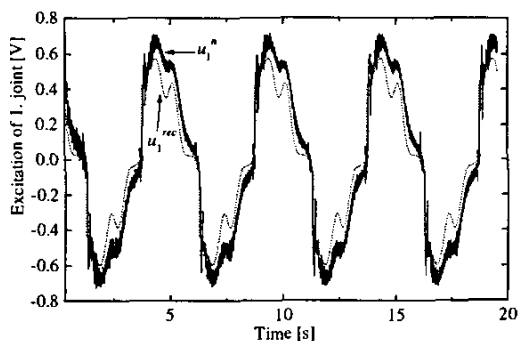

Fig. 10. Experimental (solid) and reconstructed (dotted) excitation of the first joint

Although it is possible to improve the accuracy in reconstruction of the control voltages, it is already good enough for implementation in model-based control algorithms. The identified model can adequately compensate for nonlinear dynamic effects, such as Coriolis/centripetal, gravitational and friction forces, and in turn relax demands on the controllers in the feedback loops. In the case of the available laboratory set-up (Fig. 1), motion controllers are implemented in Simulink [2]. This means that, for example, identical Simulink block diagram used for simulation of the LuGre friction model (9) is also used for real-time application. Integration of (9) is performed using Matlab routine 'ode45'.

Our current efforts are dedicated towards overcoming the problems of position dependent friction, cogging, and dynamics of the actuators. Under consideration is also an extension of the dynamic model that takes into account interaction of robot's tip with the environment (impact of outer forces/torques, as well as influence of dynamic load).

5. Conclusion

In this paper we present a systematic procedure for identification of the RRR robot dynamic model. The procedure begins with a derivation of the model in symbolic form, which is then represented in a liner form with respect to the minimum number of identifiable dynamic parameters. To improve a realistic behavior of the model, friction effects are described using the LuGre model. However, this model does not have a linear parameterization and can not be combined with the dynamic model for simultaneous estimation of both dynamic and friction coefficients. We show that it is possible

to estimate parameters of the friction model for each joint prior to estimation of the dynamic parameters. To improve the procedures for estimation of the friction parameters, we suggest an elegant and efficient algorithm in two steps. First, instead of a time demanding sequence of experiments that estimate the pre-sliding friction parameters, we suggest the use of an augmented state extended Kalman filter. Then, a frequency-domain method is used for identification of sliding friction parameters. The estimated friction models (for each joint individually) give an adequate reconstruction of friction effects, which is verified in simulations and in experiments. These models are used to extract friction effects from experimental excitations, in order to determine the part of the control signals corresponding to the robot dynamics with actuators. That part is used to estimate elements of the minimum set of identifiable parameters, which can be performed using the least-squares method. The estimated model satisfactorily covers experimental results. It can be used in model-based control laws.

References

[1] B. van Beek, B. de Jager, "RRR-Robot Design: Basic Outlines, Servo Sizing, and Control," *Proc. IEEE Int. Conf. Control Applications*, pp. 36-41, Hartford, USA, 1997.

[2] B. van Beek, B. de Jager, "An experimental facility for nonlinear robot control," *Proc. IEEE Int. Conf. Control Applications*, pp. 668-673, Hawai'i, USA, 1999.

[3] M. Vukobratović, V. Potkonjak, *Dynamics of Manipulation Robots: Theory and Application*, Springer-Verlag, Berlin, 1982.

[4] H. Olsson, K.J. Åström, C.C. de Wit, M. Gäfvert, P. Lischinsky, "Friction Models and Friction Compensation," *Eur. J. Contr.*, Vol. 4, No. 3, pp. 176-195, 1998.

[5] C.C. de Wit; H. Olsson, K.J. Åström, P. Lischinsky, "A new model for control of systems with friction," *IEEE Trans. on Autom. Control.*, Vol. 40, No. 3, pp. 419-425, 1995.

[6] R.H.A. Hensen, G.Z. Angelis, M.J.G. van de Molengraft, A.G. de Jager, J.J. Kok, "Grey-box modelling of friction: An experimental case study," *Europ. J. Contr.*, Vol. 6, No.3, pp. 258-267, 2000.

[7] R.H.A. Hensen, M.J.G. van de Molengraft, M. Steinbuch, "Frequency Domain Identification of Dynamic Friction Model Parameters," *IEEE Trans. on Contr. Syst. Tech.*, scheduled for publication in 2001.

[8] K.S. Fu, R.C. Gonzales, C.S.G. Lee, *Robotics: Control, sensing, vision, and intelligence*, McGraw-Hill Book Comp., 1987.

[9] H. Mayeda, K. Yoshida, K. Osuka, "Base Parameters of Manipulator Dynamic Models," *IEEE Trans. on Rob. and Autom.*, Vol. 6, No. 3, pp. 312-321, 1990.

[10] J. Swevers, C. Ganseman, D.B. Tukel, J. de Schutter, H. van Brussel, "Optimal Robot Excitation and Identification," *IEEE Trans. on Rob. and Autom.*, Vol. 13, No. 5, pp. 730-740, 1997.

[11] G. Calafiore, M. Indri, B. Bona, "Robot Dynamic Calibration: Optimal Excitation Trajectories and Experimental Parameter Estimation," *J. Rob. Syst.*, Vol. 18, No. 2, pp. 55-68, 2001.

[12] A. Gelb, *Applied Optimal Estimation*, M.I.T. Press, 1996.

[13] P.I. Corke, "A Robotics Toolbox for Matlab," *IEEE Robot. Autom. Mag.*, Vol. 3, No. 1, pp. 24-32, 1996.

[14] G.H. Golub, C.F. van Loan, *Matrix Computations*, John Hopkins Univ. Press, 1996.